

Theory for magnetic-field-driven 3D metal-insulator transitions in the quantum limit

Peng-Lu Zhao,¹ Hai-Zhou Lu,^{1,2,*} and X. C. Xie^{3,4,5}

¹Shenzhen Institute for Quantum Science and Engineering and Department of Physics, Southern University of Science and Technology (SUSTech), Shenzhen 518055, China

²Shenzhen Key Laboratory of Quantum Science and Engineering, Shenzhen 518055, China

³International Center for Quantum Materials, School of Physics, Peking University, Beijing 100871, China

⁴CAS Center for Excellence in Topological Quantum Computation, University of Chinese Academy of Sciences, Beijing 100190, China

⁵Beijing Academy of Quantum Information Sciences, West Building 3, No. 10, Xibeiwang East Road, Haidian District, Beijing 100193, China

(Dated: January 27, 2023)

Metal-insulator transitions driven by magnetic fields have been extensively studied in 2D, but a 3D theory is still lacking. Motivated by recent experiments, we develop a scaling theory for the metal-insulator transitions in the strong-magnetic-field quantum limit of a 3D system. By using a renormalization-group calculation to treat electron-electron interactions, electron-phonon interactions, and disorder on the same footing, we obtain the critical exponent that characterizes the scaling relations of the resistivity to temperature and magnetic field. By comparing the critical exponent with those in a recent experiment [Tang et al., Nature 569, 537 (2019)], we conclude that in which the insulating ground state was not only a charge density wave driven by electron-phonon interactions but also coexisting with strong electron-electron interactions and back-scattering disorder. Our theory will be helpful for exploring the emergent territory of 3D metal-insulator transitions under strong magnetic fields.

Introduction.—Metal-insulator transition is a fascinating problem in condensed matter physics because of its rich mechanisms [1]. There have been extensive studies on 2D metal-insulator transitions in magnetic fields [1–16], but a 3D theory is still lacking, despite that the recent experiments show that magnetic fields can drive metal-insulator transitions in 3D systems [17–21] with characteristics of quantum phase transitions [22–24], in particular in the strong-field quantum limit of a topological insulator [20, 21]. It is challenging to determine the insulating ground states in strong magnetic fields, because magnetic fields reduce the effective dimension, leading to stronger interactions and related instabilities, such as charge or spin density wave, Wigner crystal, Anderson localization, etc [24–30].

In this Letter we develop a scaling theory for the metal-insulator transition in the quantum limit of a 3D topological insulator under strong magnetic fields. Our theory agrees well with the recent experiments [20]. The quantum phase transition is governed by universal relations described by critical exponents [22] [Fig. 1(a)], corresponding to various instabilities and universal classes [24, 28, 31–36]. With the help of a renormalization-group calculation, we find the dynamical critical exponents z and correlation length exponents ν for the candidate instabilities. Based on them, we build the scaling relations of the resistivity to temperature and magnetic field, described by a critical exponent ξ . We find ξ for five cases [Tab. I]. By comparing with the experimentally measured $\xi = 5.5$ [20], we conclude that the insulating ground state is a charge density wave not only driven by electron-phonon interactions but also requiring strong electron-electron interactions and back-scattering disorder. Our

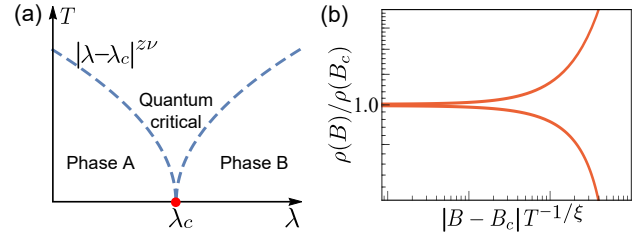


FIG. 1. (a) A quantum phase transition can be described by a non-thermal parameter λ that converges to λ_c at the quantum critical point. The boundaries (dashed curves) of the quantum critical region are described by $T \propto |\lambda - \lambda_c|^{z\nu}$, where z is the dynamical critical exponent and ν is the correlation length exponent. (b) The magnetic field B can serve as λ , and z and ν can be used to construct a measurable critical exponent ξ that describes the resistivity as a scaling function of magnetic field and temperature, e.g., $\rho(B)/\rho(B_c) = f(|B - B_c|/T^{1/\xi})$, where $f(x)$ is a scaling function with $f(0) = 1$.

theory will be helpful for the emergent territory of 3D metal-insulator transitions under strong magnetic fields.

Model for 3D systems in strong fields.—3D insulators and metals can be generically described by a Dirac model [37]

$$\mathcal{H} = m(\mathbf{k})\tau_z\sigma_0 + v_x k_x \tau_x \sigma_z + v_y k_y \tau_y \sigma_0 + v_z k_z \tau_x \sigma_x, \quad (1)$$

where $\mathbf{k} = (k_x, k_y, k_z)$ is the wave vector, τ and σ are Pauli matrices for pseudo and real spin, respectively, $v_{x,y,z}$ are parameters for the “Fermi velocities”, and $m(\mathbf{k})$ stands for the “Dirac mass” [38]. We will focus on the quantum limit in strong fields, where a z -direction magnetic field splits the energy spectrum into a series of 1D bands of Landau levels dispersing with

TABLE I. Comparison between experiments [20] and our theory on the critical exponent ξ that describes the scaling relations of the resistivity to temperature and magnetic field, for different dominant and coexisting interactions and disorder. In the experiments, the metal-insulator transition happens at a critical magnetic field of $B_c = 6.71$ T, where an incommensurate charge density wave dominates the ground state according to our theory.

Phases	Dominant	Coexisting	ξ
Charge density wave	Electron-phonon	Electron-electron	1.5
Anderson localization	Forward-scattering disorder	Electron-phonon Electron-electron	2
Charge density wave	Electron-phonon	Back-scattering disorder Weak electron-electron	4.5
Wigner crystal	Electron-electron	Back-scattering disorder Electron-electron	2
Charge density wave	Electron-phonon	Back-scattering disorder Strong electron-electron	6

Experiment						
Sample	1	2	3	4	Mean value (all samples)	Mean value (2,3,4)
ξ	3.95	6.06	5.78	6.25	5.5 ± 1.1	6.0 ± 0.1

k_z and only the lowest Landau band 0+ is occupied [Fig. 2]. An effective free Hamiltonian for the lowest Landau band can be found by linearizing the dispersion near the two Fermi wave vectors $\pm k_F \mathbf{e}_z$ [Fig. 2(b)] as $H_0 = \sum_{\mathbf{k}} \psi^\dagger(\mathbf{k}) v_F k_z \sigma_z \psi(\mathbf{k})$ [39], where $\psi(\mathbf{k}) = (\psi_-(\mathbf{k}), \psi_+(\mathbf{k}))^T$, $\psi_\pm^\dagger(\mathbf{k})$ and $\psi_\pm(\mathbf{k})$ are the creation and annihilation operators near $\mp k_F$, and \mathbf{k} is measured from $\pm k_F \mathbf{e}_z$.

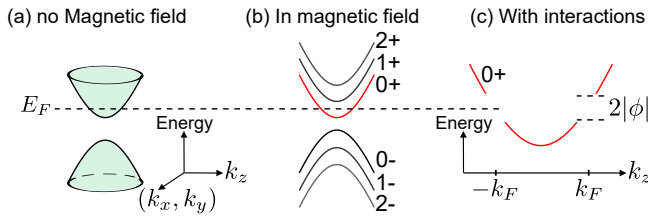


FIG. 2. A z -direction magnetic field splits the energy spectrum of a 3D insulator or metal (a) into 1D bands of Landau levels dispersing with the wave vector k_z (b). The $n\pm$ stand for the n -th Landau bands. In the quantum limit, the Fermi energy E_F crosses the lowest Landau band 0+ at $\pm k_F$. (c) Correlations between electrons near $-k_F$ and k_F open a gap of size $2|\phi|$.

Interactions and disorder.—Electron-electron or electron-phonon interactions can open a charge density wave gap near $\pm k_F$ [see Fig. 2(c)]. The charge density wave may induce the Wigner crystal [25, 26]. Also,

disorder could induce the Anderson localization [27, 28]. We study them on the same footing by using the effective action

$$S = \int d^3x d\tau (\mathcal{L}_e + \mathcal{L}_p + \mathcal{L}_b) + \int d^3x d\tau d\tau' \mathcal{L}_d, \quad (2)$$

$$\mathcal{L}_e = u \psi_+^\dagger \psi_+ \psi_-^\dagger \psi_-, \quad \mathcal{L}_p = g(\phi \psi_+^\dagger \psi_- + \phi^* \psi_-^\dagger \psi_+),$$

$$\mathcal{L}_b = |\partial_\tau \phi|^2 + v_b^2 |\boldsymbol{\partial} \phi|^2 + r |\phi|^2,$$

$$\mathcal{L}_d = - \sum_{i=f,b} (\Delta_i/2) (\psi^\dagger \Gamma_i \psi)_\tau (\psi^\dagger \Gamma_i \psi)_{\tau'}.$$

The Lagrangian \mathcal{L}_e describes electron-electron interactions that induce the $2k_F$ -instability [40]. \mathcal{L}_p represents the coupling between charge density wave order parameter ϕ and electrons [30, 41, 42]. The order parameter is defined as $\phi = (\alpha_{2k_F}/V) (\langle b_{-2k_F \mathbf{e}_z}^\dagger \rangle + \langle b_{2k_F \mathbf{e}_z} \rangle)$, where $b_{\mathbf{q}}^\dagger$, $b_{\mathbf{q}}$ are the creation and annihilation operators for the phonons with momentum \mathbf{q} , and α_q measures the electron-phonon coupling strength [41, 42]. \mathcal{L}_b describes the order parameter dynamics [23] with $r = 0$ at the quantum critical point. \mathcal{L}_d is the Lagrangian of disorder after being ensemble-averaged by means of the replica method [43–45]. The Hamiltonian of disorder takes the form $\mathcal{H}_{\text{dis}} = U_i(x) \psi^\dagger \Gamma_i \psi$, where $U_i(x)$ is the impurity potential of a Gaussian white-noise distribution as $\langle U_i \rangle = 0$ and $\langle U_i(\mathbf{x}) U_j(\mathbf{x}') \rangle = \Delta_i \delta_{ij} \delta(\mathbf{x} - \mathbf{x}')$. For the forward-scattering disorder, $\Gamma_i = \sigma_0$, which couples electrons near k_F only to k_F or $-k_F$ only to $-k_F$ [29, 46], which may induce the Anderson localization. For the back-scattering disorder, $\Gamma_i = \sigma_x + \sigma_y$, which couples electrons near k_F to $-k_F$ or $-k_F$ to k_F [29, 46]. We study these two types of disorder separately.

Renormalization-group equations.—The renormalization group [47–50] is an approach to determine the instabilities and corresponding critical exponents. We perform a Wilsonian momentum-shell renormalization-group analysis [51] for the model described above. The momentum shell is defined as $e^{-\ell} \Lambda < |\mathbf{k}_z| < \Lambda$, where ℓ is the running scale parameter. The renormalization-group flow equations are found as [39]

$$dv_F/d\ell = [z - 1 + 2\beta\gamma^3/(\gamma + 1)^2 - a_{1i}\Delta_i]v_F,$$

$$d\Delta_f/d\ell = 2\Delta_f^2 + \Delta_f - 4\beta\gamma^3\Delta_f/(\gamma + 1)^2,$$

$$d\Delta_b/d\ell = -4\Delta_b^2 + (1 + 2u)\Delta_b - \frac{2\beta\gamma^2(2\gamma + 1)\Delta_b}{(\gamma + 1)^2},$$

$$d\beta/d\ell = -2\beta^2\gamma^2/(\gamma + 1)^2 + (2 + 2u - 2a_{2i}\Delta_i)\beta,$$

$$du/d\ell = 2u^2 - 2\beta\gamma^2u/(\gamma + 1) - a_{3i}\Delta_iu, \quad (3)$$

where a_{mi} is a 3×2 constant matrix with elements $a_{mi} = (m, 2)$, and $i = f, b$ representing the forward- and backward-scattering disorder, respectively. z is the dynamic exponent, which can be found by fixing v_F . We

have redefined the dimensionless coupling constants as

$$\begin{aligned} \text{Electron-phonon: } & g^2/4\pi^2\ell_B^2v_b^3\Lambda^2 \rightarrow \beta, \\ \text{Electron-electron: } & u/4\pi^2v_F\ell_B^2 \rightarrow u, \\ \text{Disorder: } & \Delta_i/2\pi^2v_F^2\ell_B^2\Lambda \rightarrow \Delta_i, \end{aligned} \quad (4)$$

where ℓ_B is the magnetic length. Quite different from non-magnetic field theories, the integrals in the plain take into account the Landau degeneracy of the magnetic field [39]. The renormalization-group equations highly depend on the parameter $\gamma \equiv |v_b/v_F|$, the ratio of the phonon speed to the Fermi velocity, which does not flow with ℓ , and $\gamma \approx 1.7 \times 10^{-3}$ from the model parameters [39]. Later, our conclusions hold for a range of small γ .

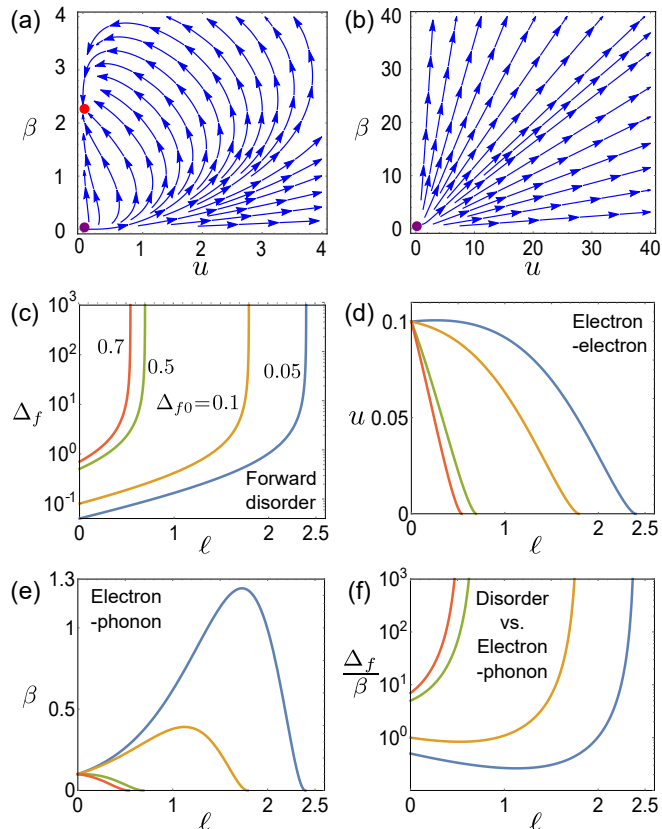


FIG. 3. The renormalization-group flow in the u - β plane for (a) $\gamma = 2$, (b) $\gamma = 0.002$. u and β measure the effective electron-electron and electron-phonon interactions, respectively. $\gamma = |v_b/v_F|$ is the ratio of the phonon speed to Fermi velocity. There are two fixed points at $(i)_c (u_*, \beta_*) = (0, 0)$ and $(ii)_c (0, (1 + 1/\gamma)^2)$. (c)-(f) Flows of Δ_f , u , β , and Δ_f/β , as functions of the running scale parameter ℓ , for different initial value Δ_{f0} of Δ_f . Δ_f measures the forward-scattering disorder. We fix the initial values of u and β at $u_0 = \beta_0 = 0.1$. (c)-(f) share the same legends.

Charge density wave without disorder?—For a system with only electron-electron and electron-phonon interactions, there are two fixed points [Fig. 3(a)] at $(i)_c (u_*, \beta_*) = (0, 0)$ and $(ii)_c (0, (1 + 1/\gamma)^2)$. If phonon-Fermi velocity ratio is not extremely small (e.g., $\gamma > 1$),

the attractive fixed point $(ii)_c$ [39] has a small value for electron-phonon interactions. Neither electron-electron nor electron-phonon interactions could induce the charge density wave. This conclusion explicitly conflicts with the Peierls phase transition [30]. Due to an extremely small γ , the attractive fixed point $(ii)_c$ behaves like an infinitely large electron-phonon coupling point. Before reaching the attractive point $(ii)_c$, the electron-phonon coupling becomes strong enough to induce the Peierls phase transition which opens a charge-density-wave gap. Therefore, an extremely small γ is crucial to induce the Peierls phase transition. In this case, electron-phonon interactions can be viewed as a perturbation starting from the Gaussian fixed point $(i)_c$ [see Fig. 3(b)]. The linearized renormalization-group equations around the fixed point $(i)_c$ show that the electron-phonon coupling increases with ℓ as $e^{2\ell}$. Therefore, the correlation length diverges with an exponent $\nu_\beta = 1/2$ and the dynamical critical exponent $z = 1$ [39]. The general scaling relation of the resistivity to temperature and magnetic field is given by [1, 52, 53]

$$\rho(B, T) = \rho(B_c) f[|B - B_c|/T^{1/z\nu_B}], \quad (5)$$

where $f(x)$ is a scaling function with $f(0) = 1$. Our scaling analysis yields $\nu_B = 3\nu_\beta$ [39], and the critical exponent takes the form

$$\xi = 3z\nu_\beta = 1.5. \quad (6)$$

This value is far less than the experimental value $\xi = 5.5$ [20], so without disorder, the coexistence of electron-electron and electron-phonon interactions cannot induce the metal-insulator transitions in the experiments [20].

Anderson localization induced by forward-scattering disorder?—When the forward-scattering disorder coexists with electron-phonon interactions and electron-electron interactions, there are two fixed points at $(i)_f (u_*, \beta_*, \Delta_f^*) = (0, 0, 0)$ and $(ii)_f (0, (1 + 1/\gamma)^2, 0)$. The fixed points for the forward-scattering disorder are always zero and unstable [39]. Figure 3(c) shows that the disorder coupling will flow to infinity with increasing ℓ , no matter how small its initial value is. This means that any weak forward-scattering disorder induces the Anderson localization. Considering that $u_* = 0$ is stable [see Fig. 3(d)], fixed point $(i)_f$ is a multi-critical point for the charge density wave and Anderson localization. The competition of the two phases leads to a suppression of the charge density wave by the Anderson localization. Figure 3(e) shows that β first increases with increasing ℓ then decays to zero rapidly when the initial value of Δ_f is very small, or flows to zero without the increase if the initial value of Δ_f is large enough. To distinguish which coupling is dominant, Fig. 3(f) shows the ratio of $\Delta_f(\ell)$ to $\beta(\ell)$, which grows rapidly with increasing ℓ . Due to the suppression of the charge density wave, the correlation length exponent is obtained from the divergent disorder coupling, which gives a correlation length

exponent as $\nu_\Delta = 1$ [39]. The dynamical critical exponent is $z = 1 + \Delta_f^* = 1$ with $\Delta_f^* = 0$, the scaling analysis means that $\nu_B = 2\nu_\Delta$ [39]. The critical exponent is

$$\xi = 2z\nu_\Delta = 2, \quad (7)$$

still far less than the experimental value $\xi = 5.5$ [20], so the interplay of electron-phonon, electron-electron interactions and forward-scattering disorder cannot induce the metal-insulator transition in the experiments [20], where the insulating ground state is not an Anderson insulator.

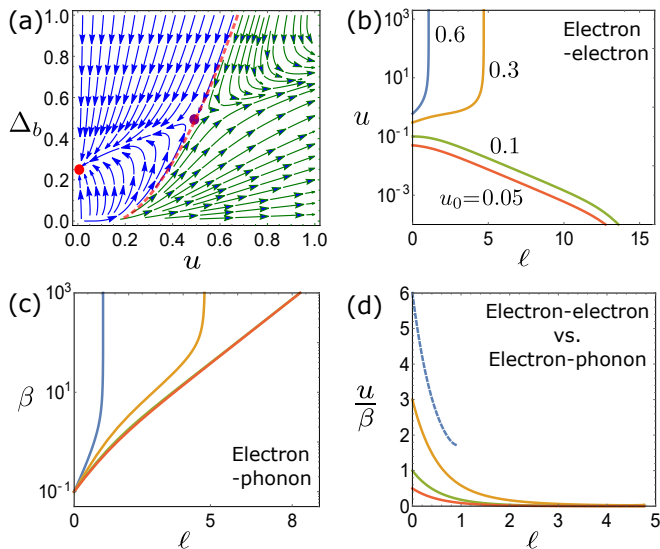


FIG. 4. (a) The renormalization-group flow in the u - Δ_b plane, in absence of the electron-phonon coupling. In this case, there are two non-Gaussian fixed points at $(u_*, \Delta_b^*) = (0, 1/4)$ and $(1/2, 1/2)$. The red curve distinguishes a disordered metal with zero electron-electron coupling on the left and a Wigner crystal on the right. (b)-(d) Running of the electron-electron coupling u , electron-phonon coupling β , and u/β with ℓ , for different initial values of u . The initial values of both Δ_b and β are 0.1. (c)-(d) share the same legends. The green and red lines overlap in (c).

Charge density wave induced by back-scattering disorder.—When the back-scattering disorder exists, the fixed points are (i)_b $(u_*, \beta_*, \Delta_b^*) = (0, 0, 0)$; (ii)_b $(0, (1 + 1/\gamma)^2, 0)$; (iii)_b $(0, 0, 1/4)$; and (iv)_b $(1/2, 0, 1/2)$, belonging to four different universality classes because they have different critical exponents. Fixed point (i)_b is unstable for electron-phonon interactions and disorder. Fixed point (ii)_b is attractive for all three couplings and represents the charge density wave with an irrelevant electron-electron coupling and back-scattering disorder. Without electron-phonon interactions, fixed point (iii)_b is stable and fixed point (iv)_b is a critical point for a Wigner crystal. As shown in Fig. 4(a), there exists a critical line in the u - Δ_b plane, on the right, u flows to infinity, indicating a charge density wave driven by electron-electron interactions, i.e., a Wigner crystal,

while on the left, the system flows to a finite disorder fixed point with a stable zero-valued electron-electron coupling. When including electron-phonon interactions, as shown in Fig. 4(b), the behavior of u does not change qualitatively. Figure 4(c) shows that the electron-phonon coupling β flows to infinity with increasing ℓ . Near fixed point (iii)_b, β is the only unstable coupling. Fixed point (iii)_b becomes the critical fixed point for a charge density wave induced by electron-phonon interactions in the presence of a finite back-scattering disorder and irrelevant electron-electron coupling. The divergent β gives $\nu_\beta = 1$ [39]. The dynamical critical exponent for this universality class is found as $z = 1 + 2\Delta_b^* = 1.5$. We thus get a critical exponent for the resistivity scaling

$$\xi = 3z\nu_\beta = 4.5, \quad (8)$$

which is close to the experimental value $\xi = 5.5$ [20].

Near fixed point (iv)_b, both β and u are unstable and increase unboundedly when the initial value of u is large enough. Fixed point (iv)_b is a multi-critical point for the Wigner crystal or Peierls phase transition. Which phase transition occurs first depends on the relative strength of β and u . The solid lines in Fig. 4(d) show that the ratio of u to β decreases rapidly and finally vanishes when its initial value is not large enough, indicating that the Peierls phase transition happens first. However, the dotted line in Fig. 4(d) shows that u is always larger than β , when its initial value is large enough, which means that the Wigner crystal occurs first. Despite that these two phase transitions both produce charge density waves, the gap sizes and critical behaviors are different [29, 30]. For the Peierls phase transition, the correlation length exponent is $\nu_\beta = 1$ and the dynamical critical exponent is $z = 1 + 2\Delta_b^* = 2$, which gives a critical exponent for the resistivity scaling

$$\xi = 3z\nu_\beta = 6. \quad (9)$$

For the Wigner crystal, we obtain $\nu_u = 1$ and $z = 2$, which lead to $\xi = 2$ [39].

Conclusion and discussion.—So far, $\xi = 6$ is closest to the experimental result $\xi = 5.5$ [20]. Therefore, we conclude that the magnetic-field-induced metal-insulator transition in the experiments is likely a charge density wave induced by electron-phonon interactions, in the presence of strong electron-electron interactions and back-scattering disorder. Its quantum critical behavior is described by the universal class of fixed point (iv)_b with a correlation length exponent $\nu_B = 3$ and dynamical critical exponent $z = 2$. Our theory provides a deeper understanding to the data in Ref. [20], where the value $\xi = 5.5$ is obtained by averaging four samples, as shown in Tab. I. However, the value of ξ for samples 1 is closer to the value $\xi = 4.5$ of the universal class described by fixed point (iii)_b. By contrast, ξ of samples 2-4 belong to fixed point (iv)_b. The physical difference is that electron-electron interactions in sample 1 can be seen as zero-valued when

the metal-insulator transition happens whereas it is finite and strong in other three samples. As shown in Tab. I, the mean value of samples 2-4 gives rise to $\xi = 6.0$, which remarkably agrees with our theoretical value in Eq. (9). Despite that we take the experiments in Ref. [20] as a concrete sample to compare with, our theory can be applied to other 3D metal-insulator transitions under strong magnetic fields, such as those in layered structures HfTe_5 [21]. Nevertheless, 3D metal-insulator transitions of spin-correlated systems driven by magnetic fields [17–19] are beyond the scope of our theory and will be a challenging topic in the future.

We thank helpful discussions with Liyuan Zhang and Tingyu Gao. This work was supported by the National Natural Science Foundation of China (11534001, 11974249, and 11925402), the Strategic Priority Research Program of Chinese Academy of Sciences (XDB28000000), Guangdong province (2016ZT06D348, 2020KCXTD001), the National Key R & D Program (2016YFA0301700), Shenzhen High-level Special Fund (G02206304, G02206404), and the Science, Technology and Innovation Commission of Shenzhen Municipality (ZDSYS20170303165926217, JCYJ20170412152620376, KYTDPT20181011104202253). The numerical calculations were supported by Center for Computational Science and Engineering of SUSTech.

* Corresponding author: luhz@sustech.edu.cn

- [1] Masatoshi Imada, Atsushi Fujimori, and Yoshinori Tokura, “Metal-insulator transitions,” *Rev. Mod. Phys.* **70**, 1039–1263 (1998).
- [2] D J Newson and M Pepper, “Critical conductivity at the magnetic-field-induced metal-insulator transition in n-GaAs and n-InSb,” *J. Phys. C* **19**, 3983–3990 (1986).
- [3] V. J. Goldman, M. Shayeghan, and H. D. Drew, “Anomalous Hall Effect below the Magnetic-Field-Induced Metal-Insulator Transition in Narrow-Gap Semiconductors,” *Phys. Rev. Lett.* **57**, 1056–1059 (1986).
- [4] M. C. Maliepaard, M. Pepper, R. Newbury, J. E. F. Frost, D. C. Peacock, D. A. Ritchie, G. A. C. Jones, and G. Hill, “Evidence of a magnetic-field-induced insulator-metal-insulator transition,” *Phys. Rev. B* **39**, 1430–1433 (1989).
- [5] Peihua Dai, Youzhu Zhang, and M. P. Sarachik, “Effect of a magnetic field on the critical conductivity exponent at the metal-insulator transition,” *Phys. Rev. Lett.* **67**, 136–139 (1991).
- [6] Steven Kivelson, Dung-Hai Lee, and Shou-Cheng Zhang, “Global phase diagram in the quantum Hall effect,” *Phys. Rev. B* **46**, 2223–2238 (1992).
- [7] T. Wang, K. P. Clark, G. F. Spencer, A. M. Mack, and W. P. Kirk, “Magnetic-field-induced metal-insulator transition in two dimensions,” *Phys. Rev. Lett.* **72**, 709–712 (1994).
- [8] Y. Tomioka, A. Asamitsu, H. Kuwahara, Y. Moritomo, and Y. Tokura, “Magnetic-field-induced metal-insulator phenomena in $\text{Pr}_{1-x}\text{Ca}_x\text{MnO}_3$ with controlled charge-ordering instability,” *Phys. Rev. B* **53**, R1689–R1692 (1996).
- [9] Dragana Popović, A. B. Fowler, and S. Washburn, “Metal-Insulator Transition in Two Dimensions: Effects of Disorder and Magnetic Field,” *Phys. Rev. Lett.* **79**, 1543–1546 (1997).
- [10] X. C. Xie, X. R. Wang, and D. Z. Liu, “Kosterlitz-Thouless-Type Metal-Insulator Transition of a 2D Electron Gas in a Random Magnetic Field,” *Phys. Rev. Lett.* **80**, 3563–3566 (1998).
- [11] Jin An, C. D. Gong, and H. Q. Lin, “Theory of the magnetic-field-induced metal-insulator transition,” *Phys. Rev. B* **63**, 174434 (2001).
- [12] H. Kempa, P. Esquinazi, and Y. Kopelevich, “Field-induced metal-insulator transition in the c-axis resistivity of graphite,” *Phys. Rev. B* **65**, 241101 (2002).
- [13] E. V. Gorbar, V. P. Gusynin, V. A. Miransky, and I. A. Shovkovy, “Magnetic field driven metal-insulator phase transition in planar systems,” *Phys. Rev. B* **66**, 045108 (2002).
- [14] Y. Kopelevich, J. C. Medina Pantoja, R. R. da Silva, and S. Moehlecke, “Universal magnetic-field-driven metal-insulator-metal transformations in graphite and bismuth,” *Phys. Rev. B* **73**, 165128 (2006).
- [15] D. J. W. Geldart and D. Neilson, “Quantum critical behavior in the insulating region of the two-dimensional metal-insulator transition,” *Phys. Rev. B* **76**, 193304 (2007).
- [16] S V Kravchenko and M P Sarachik, “Metal-insulator transition in two-dimensional electron systems,” *Rep. Prog. Phys.* **67**, 1–44 (2003).
- [17] S. Calder, V. O. Garlea, D. F. McMorrow, M. D. Lumsden, M. B. Stone, J. C. Lang, J.-W. Kim, J. A. Schlueter, Y. G. Shi, K. Yamaura, Y. S. Sun, Y. Tsujimoto, and A. D. Christianson, “Magnetically Driven Metal-Insulator Transition in NaOsO_3 ,” *Phys. Rev. Lett.* **108**, 257209 (2012).
- [18] K. Ueda, J. Fujioka, B.-J. Yang, J. Shiogai, A. Tsukazaki, S. Nakamura, S. Awaji, N. Nagaosa, and Y. Tokura, “Magnetic Field-Induced Insulator-Semimetal Transition in a Pyrochlore $\text{Nd}_2\text{Ir}_2\text{O}_7$,” *Phys. Rev. Lett.* **115**, 056402 (2015).
- [19] Zhaoming Tian, Yoshimitsu Kohama, Takahiro Tomita, Hiroaki Ishizuka, Timothy H. Hsieh, Jun J. Ishikawa, Koichi Kindo, Leon Balents, and Satoru Nakatsuji, “Field-induced quantum metal-insulator transition in the pyrochlore iridate $\text{Nd}_2\text{Ir}_2\text{O}_7$,” *Nat. Phys.* **12**, 134–138 (2016).
- [20] Fangdong Tang, Yafei Ren, Peipei Wang, Ruidan Zhong, John Schneeloch, Shengyuan A. Yang, Kun Yang, Patrick A. Lee, Genda Gu, Zhenhua Qiao, and Liyuan Zhang, “Three-dimensional quantum Hall effect and metal-insulator transition in ZrTe_5 ,” *Nature* **569**, 537–541 (2019).
- [21] Peng Wang, Yafei Ren, Fangdong Tang, Peipei Wang, Tao Hou, Hualing Zeng, Liyuan Zhang, and Zhenhua Qiao, “Approaching three-dimensional quantum Hall effect in bulk HfTe_5 ,” *Phys. Rev. B* **101**, 161201(R) (2020).
- [22] Matthias Vojta, “Quantum phase transitions,” *Rep. Prog. Phys.* **66**, 2069–2110 (2003).
- [23] Subir Sachdev, *Quantum Phase Transitions*, 2nd ed. (Cambridge University Press, 2011).
- [24] Hilbert v. Löhneysen, Achim Rosch, Matthias Vojta, and Peter Wölfle, “Fermi-liquid instabilities at magnetic

- quantum phase transitions,” *Rev. Mod. Phys.* **79**, 1015–1075 (2007).
- [25] E. Wigner, “On the Interaction of Electrons in Metals,” *Phys. Rev.* **46**, 1002–1011 (1934).
- [26] Stuart B. Field, D. H. Reich, B. S. Shivaram, T. F. Rosenbaum, D. A. Nelson, and P. B. Littlewood, “Evidence for depinning of a Wigner crystal in Hg-Cd-Te,” *Phys. Rev. B* **33**, 5082–5085 (1986).
- [27] P. W. Anderson, “Absence of Diffusion in Certain Random Lattices,” *Phys. Rev.* **109**, 1492–1505 (1958).
- [28] E. Abrahams, P. W. Anderson, D. C. Licciardello, and T. V. Ramakrishnan, “Scaling theory of localization: Absence of quantum diffusion in two dimensions,” *Phys. Rev. Lett.* **42**, 673–676 (1979).
- [29] T. Giamarchi, *Quantum Physics in One Dimension* (Clarendon Press, 2003).
- [30] G. Grüner, *Density Waves in Solids* (Westview Press, 2000).
- [31] Franz J. Wegner, “Electrons in disordered systems. Scaling near the mobility edge,” *Z. Phys. B* **25**, 327–337 (1976).
- [32] W. L. McMillan, “Scaling theory of the metal-insulator transition in amorphous materials,” *Phys. Rev. B* **24**, 2739–2743 (1981).
- [33] C. A. Stafford and A. J. Millis, “Scaling theory of the Mott-Hubbard metal-insulator transition in one dimension,” *Phys. Rev. B* **48**, 1409–1425 (1993).
- [34] Bodo Huckestein, “Scaling theory of the integer quantum Hall effect,” *Rev. Mod. Phys.* **67**, 357–396 (1995).
- [35] V. Dobrosavljević, Elihu Abrahams, E. Miranda, and Sudip Chakravarty, “Scaling Theory of Two-Dimensional Metal-Insulator Transitions,” *Phys. Rev. Lett.* **79**, 455–458 (1997).
- [36] Andrea Pelissetto and Ettore Vicari, “Critical phenomena and renormalization-group theory,” *Phys. Rep.* **368**, 549 – 727 (2002).
- [37] Shun-Qing Shen, *Topological Insulators*, 2nd ed. (Springer-Verlag, Berlin Heidelberg, 2017).
- [38] Y. Jiang, Z. L. Dun, H. D. Zhou, Z. Lu, K.-W. Chen, S. Moon, T. Besara, T. M. Siegrist, R. E. Baumbach, D. Smirnov, and Z. Jiang, “Landau-level spectroscopy of massive Dirac fermions in single-crystalline ZrTe₅ thin flakes,” *Phys. Rev. B* **96**, 041101(R) (2017).
- [39] See Supplemental Material for details.
- [40] Shao-Kai Jian and Zheng Zhu, “ $2k_F$ density wave instability of composite Fermi liquid,” *Phys. Rev. Res.* **2**, 033414 (2020).
- [41] H. Bruus, K. Flensberg, and Oxford University Press, *Many-Body Quantum Theory in Condensed Matter Physics: An Introduction*, Oxford Graduate Texts (OUP Oxford, 2004).
- [42] Fang Qin, Shuai Li, Z. Z. Du, C. M. Wang, Wenqing Zhang, Dapeng Yu, Hai-Zhou Lu, and X. C. Xie, “Theory for the Charge-Density-Wave Mechanism of 3D Quantum Hall Effect,” *Phys. Rev. Lett.* **125**, 206601 (2020).
- [43] Franz Wegner, “The mobility edge problem: Continuous symmetry and a conjecture,” *Z. Phys. B* **35**, 207–210 (1979).
- [44] K. B. Efetov, A. I. Larkin, and D. E. Khmel’nitskii, “Interaction of diffusion modes in the theory of localization,” *Zh. Eksp. Teor. Fiz.* **79**, 112 (1980).
- [45] Patrick A. Lee and T. V. Ramakrishnan, “Disordered electronic systems,” *Rev. Mod. Phys.* **57**, 287–337 (1985).
- [46] T. Giamarchi and H. J. Schulz, “Anderson localization and interactions in one-dimensional metals,” *Phys. Rev. B* **37**, 325–340 (1988).
- [47] Michael E. Fisher, “The renormalization group in the theory of critical behavior,” *Rev. Mod. Phys.* **46**, 597–616 (1974).
- [48] Kenneth G. Wilson, “The renormalization group and critical phenomena,” *Rev. Mod. Phys.* **55**, 583–600 (1983).
- [49] A MacKinnon, “Critical exponents for the metal-insulator transition,” *J. Phys.: Condens. Matter* **6**, 2511–2518 (1994).
- [50] H. Eugene Stanley, “Scaling, universality, and renormalization: Three pillars of modern critical phenomena,” *Rev. Mod. Phys.* **71**, S358–S366 (1999).
- [51] R. Shankar, “Renormalization-group approach to interacting fermions,” *Rev. Mod. Phys.* **66**, 129–192 (1994).
- [52] S. L. Sondhi, S. M. Girvin, J. P. Carini, and D. Shahar, “Continuous quantum phase transitions,” *Rev. Mod. Phys.* **69**, 315–333 (1997).
- [53] Matthew P. A. Fisher, “Quantum phase transitions in disordered two-dimensional superconductors,” *Phys. Rev. Lett.* **65**, 923–926 (1990).